Magnetic Resonance in Medicine 53:1166–1171 (2005)

Optimized ^{1}H MRS and MRSI Methods for the in Vivo Detection of Boronophenylalanine

Peter Bendel,[1]* Raanan Margalit,[2] and Yoram Salomon[2]

Boronophenylalanine (BPA) is used as Boron-10 carrier in boron neutron capture therapy, an experimental cancer radiotherapy. Results of quantitative, noninvasive in vivo detection and imaging of BPA in laboratory animals using ^{1}H NMR are presented for the first time. The purpose of this study was to implement and validate optimized techniques for the efficient detection of BPA. The ^{1}H NMR signals through which BPA is most readily detected in vivo are those from the aromatic ring of the molecule, which are part of a scalar-coupled spin system. The preferred detection method should therefore be based on a pulse sequence in which the effective TE is as short as possible. Modified versions of LASER (τ_{CP} = 4.6 ms, TE = 27.6 ms) and double-echo slice-selective 2D MRSI (TE = 12 ms) were implemented for single-voxel spectroscopy and spectroscopic imaging of BPA, respectively. Chemical shift selective excitation was used for both sequences, based on a pulse that enabled narrow-band excitation without concomitant delay in TE. SI data without water suppression was used for absolute quantitation and for correction of B_0 variations. Experiments were conducted at 4.7 T in phantoms and in mice where the infused BPA was detected in the kidney. Magn Reson Med 53: 1166–1171, 2005. © 2005 Wiley-Liss, Inc.

Key words: BNCT; BPA; MRS; MRSI; Chemical-shift-selective

Boron neutron capture therapy (BNCT) is a binary cancer treatment, in which ^{10}B nuclei, preferably targeted to tumors by suitable carrier molecules, are irradiated with low-energy neutrons, causing localized short-range and cell-damaging radiation (1). One of the problems confronting successful clinical implementation of BNCT is the difficulty of quantitatively mapping the distribution of the boronated (and ^{10}B-enriched) molecules in patients in the course of the treatment session. So far, MR is the only modality capable of fulfilling this task. Detection of the NMR-sensitive ^{10}B spin is the most straightforward approach to this problem, which was shown to be feasible for BSH, another molecule used in BNCT (2). However, in boronophenylalanine (BPA) the ^{10}B transverse relaxation is far more rapid than in BSH, so that direct ^{10}B detection is at much greater disadvantage compared to ^{1}H detection.

The possibility of detecting the aromatic BPA protons was recognized previously and demonstrated on a patient using standard STEAM (TE = 30 ms) (3). Subsequent studies characterized the echo-time dependence of the aromatic proton BPA signals in aqueous solutions for STEAM and PRESS sequences (4,5). As expected, these studies demonstrated the considerable modulation of the signal due to *J*-coupling, causing both phasing and signal loss problems and stressing the need for efficient, short-TE sequences.

Echo modulation by *J*-coupling can be suppressed by using very short echo times or CP-type echo trains or by timing the detection to peaks of this modulation. The latter approach is also useful for spectral editing, but for ^{1}H couplings with low *J* values, this leads to rather long echo times and signal loss from intrinsic T_2 relaxation. The use of short-TE localized MRS or SI was demonstrated for both STEAM- (6) and PRESS-based sequences (7). Sequences detecting the full Hahn spin echo have, in principle, a twofold sensitivity advantage over detection of the stimulated echo and are therefore preferred for cases such as the detection of externally administered BPA, where one strives for the highest possible sensitivity and spatial resolution.

The main purpose of this study was to design, validate, and implement single-voxel MRS and spectroscopic imaging sequences and postprocessing procedures, specifically aimed at the task of quantitatively detecting externally administered BPA. The sequence and procedure design was based on the following guidelines: (1) use of adiabatic hyperbolic secant (8) refocusing pulses with highly rectangular slice profile for volume selection, based on the LASER sequence (9); (2) use of chemical-shift-selective excitation of the spectral region encompassing only the BPA peaks of interest and basing this excitation on narrow-band pulses with minimal phase shifts for off-resonance isochromats, such as E-BURP-2 (10); (3) use of reference scans without water suppression, in which the water signal is used as intensity reference for quantitation of the BPA concentration and as B_0 reference in the postprocessing of the SI data.

METHODS

BPA

L-*p*-Boronophenylalanine at natural isotopic abundance was purchased from Katchem (Prague, Czech Republic) and used without further purification. Since the solubility of BPA is limited, solutions for administration to animals were prepared by dissolving BPA in the presence of ~15% excess of fructose, under continuous adjustment of the pH

[1]Department of Chemical Research Support, Weizmann Institute of Science, Rehovot, Israel.

[2]Department of Biological Regulation, Weizmann Institute of Science, Rehovot, Israel.

Grant sponsor: Israel Science Foundation founded by the Israel Academy of Sciences and Humanities.

*Correspondence to: Peter Bendel, Chemical Research Support Unit, MR Center, Weizmann Institute of Science, Rehovot 76100, Israel. E-mail: Peter.Bendel@weizmann.ac.il.

Received 14 September 2004; revised 2 December 2004; accepted 3 December 2004.

DOI 10.1002/mrm.20442
Published online in Wiley InterScience (www.interscience.wiley.com).

to basic conditions. The final pH of the injection solution was 8.6, and the final total BPA concentration was 0.26 M, partitioned between the BPA–fructose complex (BPA–F) and free BPA. The BPA concentration in the injection solution was determined using high-resolution ^{1}H NMR spectroscopy in which the BPA solution was diluted with a reference solution containing a known concentration of glycine in D_2O.

In Vivo Experiments

CD1 nude mice were anesthetized with a 7:3 N_2O:O_2 mixture containing 0.5–1.5% isoflurane (Medeva, Bethlehem, PA). About 1 mL of the BPA/BPA–F solution was infused through the tail vein, at a rate of about 17 μL/min for a time of ~1 h, using a Gilson Minipuls3 infusion pump (Villiers-le-Bel, France). All experiments were conducted according to Weizmann Institute guidelines (1996).

NMR Instrumentation

Phantom and in vivo experiments were conducted on a Biospec Avance system (Bruker Biospin, Ettlingen, Germany) with a 4.7-T 30-cm horizontal bore magnet. For the experiments described here, the main actively shielded 20-cm i.d. gradient coil, with maximal intensity of 100 mT/m and 0.33-ms rise time was used. The RF probe system included a 7.5-cm resonator for pulse transmission and a 2.5-cm circular receive-only surface coil, with active detuning between the transmit and receive coils.

Chemical-Shift-Selective LASER Experiments

The pulse sequence used for single-voxel spectroscopy was identical to the LASER sequence published in Ref. (9), except that the excitation pulse was replaced by a 10-ms-long 90° E-BURP-2 pulse (10). The off-resonance phase deviations over the excitation bandwidth were less than ±10°, so that, for all practical purposes, the dephasing time for the transverse magnetization can be considered to start at the end of the pulse. Volume selection in three dimensions was achieved by six 2-ms-long 180° hyperbolic secant pulses. The time between successive centers of the refocusing pulses (τ_{CP}) was 4.6 ms, so that the TE of the detected 6th echo was 27.6 ms. For in vivo experiments, spectra were typically collected with 3000 Hz spectral width, 2K points, a repetition time (TR) of 1.5 s, and 256 scans, for a total collection time of 6.4 min per spectrum. The voxel size was adjusted to the dimensions of the mouse kidney. The LASER sequence was preceded by CHESS water suppression. Reference spectra were acquired using the same pulse sequence and volume selection, but without water suppression and with the frequency of the 90° pulse centered on the water resonance, using a single scan to obtain a fully relaxed water spectrum. The BPA concentrations were calculated from the ratio between the integrals of the BPA and water signals, based on the empiric correlation obtained in phantom experiments (see below), taking into account the difference in the number of scans, as well as the expected saturation of the BPA signal.

Chemical-Shift-Selective SI Experiments

The pulse sequence for spectroscopic imaging consisted of a chemical-shift-selective E-BURP-2 pulse for excitation, followed by two slice-selective hyperbolic secant pulses for refocusing, as described for the LASER experiments, leading to TE = 12.1 ms. Phase-encode gradients along the two dimensions perpendicular to the slice selection axis were applied after the second π pulse. The sequence was preceded by water suppression, as well as by up to four spatially selective OVS pulses, for suppression of regions outside the kidney. For in vivo experiments, data were typically acquired with slice thickness of 4.5 mm, FOV of 4.5 cm, spectral width of 1800 Hz, and a 32 × 32 × 512 matrix, with TR = 1 s, and total acquisition time of 17 min. Reference data were obtained by running the same sequence without water suppression and the excitation pulse applied at the water resonance frequency.

The data were processed with phase-sensitive 3D FT using an exponential apodization filter with LB = 2 Hz along the spectral dimension. The peak positions of the phase-corrected water spectra were used to derive a map of local B_0 deviations, which were used to shift each of the spectra (both the water and the BPA data) to a common frequency scale. Integration over a spectral region of interest in the phase-corrected and frequency-aligned spectra was used to derive an intensity map for the water and BPA signals respectively. A concentration map for BPA was obtained by dividing the BPA intensity by the water intensity map, based on the empiric integral ratios obtained from phantom experiments, after correcting for the different degrees of T_1 saturation between water and BPA. All the processing after the 3D FT was performed with MATLAB.

RESULTS

Spectral Assignments

As shown by Heikkinen et al. (4), the aromatic protons in BPA–F represent a *AA′XX′* spin system, which can be approximated as a weakly coupled *AX* pair at 4.7 T. Figure 1 shows a single-voxel LASER spectrum from a phantom containing an aqueous solution of 6.5 mM total BPA at pH 8.6, indicating resolved peaks from free BPA (f) and the BPA–F complex (c). The voxel dimensions were 9 × 9 × 12 mm, and the spectrum was acquired with 256 scans and TR = 1 s. The spectrum demonstrates the lack of any phase distortion due to the short interpulse separation in the CP pulse train applied with the LASER pulse sequence.

Phantom Calibration of Concentration Determination from LASER Spectra

The integral over the aromatic BPA peaks in spectra such as shown in Fig. 1was divided by the integral over the water peak in a reference spectrum, as described under Methods. Neglecting the effect of T_2 decay, one should ideally be able to calculate the BPA concentration from

$$C_{BPA} = \frac{S_{BPA}}{S_{H_2O}} (1 - \exp(-\,TR/T_{1(BPA)})) \frac{C_{H_2O}}{2NS}, \qquad [1]$$

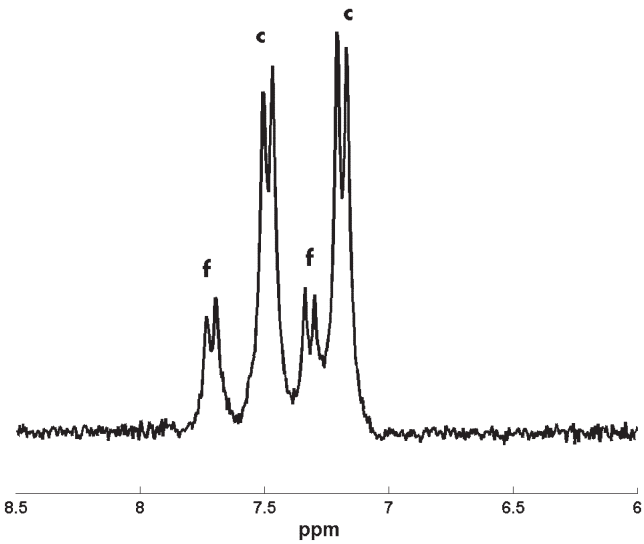

FIG. 1. LASER spectrum of 6.5 mM total BPA solution in phantom. c and f indicate signal from the BPA–F complex and free BPA, respectively. The chemical shift scale was calibrated by setting the water signal to 4.80 ppm.

where S_{BPA} and S_{H2O} are the spectral integrals of the BPA and water peaks, respectively, and NS is the number of scans used for the BPA acquisition. The division by 2 corrects for the fact that the water and BPA signals represent two versus four protons, respectively. The T_1 of the aromatic protons in BPA was 1.0 s. If the water concentration, C_{H2O}, is assumed to be 55 M, and TR = 1.5 s, then the apparent BPA concentration obtained through Eq. [1] for the 6.5 mM phantom solution was 5.8 mM. Although this discrepancy could be within the uncertainties of all the involved experimental procedures and theoretical assumptions, several calibration experiments, using different phantom solutions, all yielded a slight (~10–15%) underestimate of the true BPA concentration. A possible source of error is obviously the neglect to account for any T_2 decay effects. If one applies the intrinsic T_2 values published in Ref. (4), which were 1.07 s for water and 0.225 s for BPA (at 3 T), then the estimate for the BPA concentration in the phantom is 6.4 mM. The expected additional signal attenuation effect (for BPA) due to the scalar coupling modulation was calculated using the equations derived by Allerhand (11) and was found to be negligible (~0.3%) for the conditions applying to our experiments.

Chemical-Shift-Selective SI: Results for a Phantom

The phantom used for the experiments described in this section consisted of a cylindrical vial of 5 cm length and 15 mm i.d., filled with an aqueous solution of 65 mM total BPA, at pH 8.6. SI was performed on a 6-mm axial slice, with FOV = 4 cm, a 32 × 32 × 512 matrix, and TR = 1 s. The spectral width for these experiments was 800 Hz, so that the receiver frequency was shifted to the region of the BPA peaks for the BPA detection scan. No OVS was used in these phantom experiments.

The water and BPA intensity maps are shown in Fig. 2a and b, respectively. The intensity gradient along the vertical axis reflects the B_1 reception profile of the surface coil. This profile provides a convenient way for testing the concentration determination of the solute molecule, under conditions of varying signal intensity and S/N ratio. Thus, ideally, one expects the intensity gradient seen on the

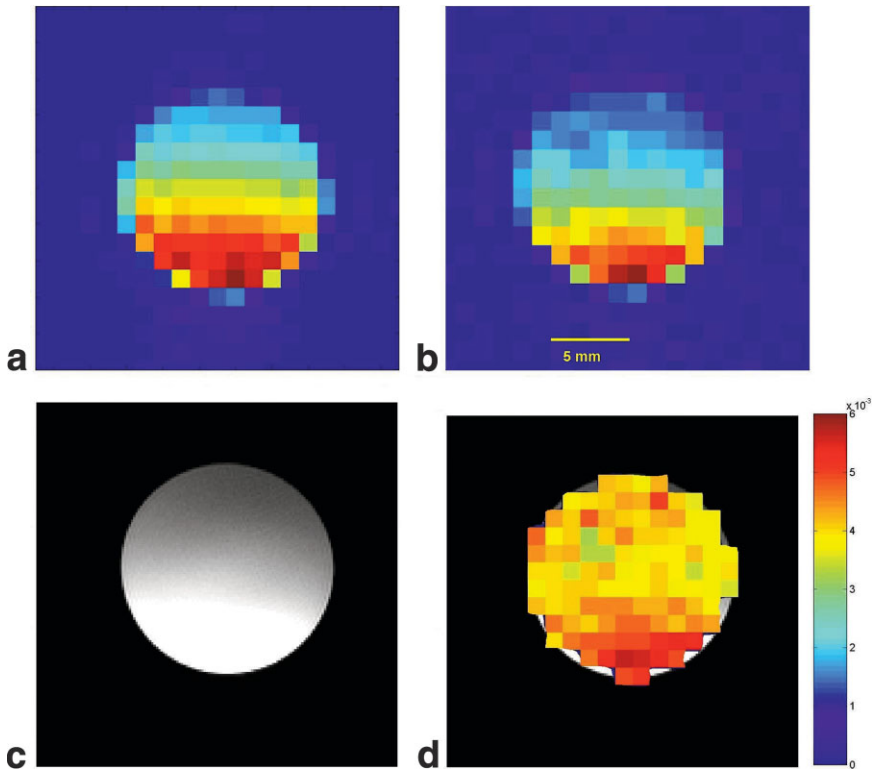

FIG. 2. (**a**). Water intensity map of the cylindrical vial phantom, derived by integrating the water peak in each of the individual voxels of the SI data. The slice thickness is 6 mm and the in-plane dimensions of each voxel is 1.25 × 1.25 mm. (**b**) BPA image of the same slice. (**c**) Spin-echo image of the slice localized and imaged in the SI phantom experiment: 256 × 256 matrix, TR = 0.6 s, TE = 16 ms, NEX = 1. (**d**) The BPA/water ratio map, superimposed on the SE image, with the ratio values range indicated on the color bar. The image was obtained by dividing the image shown in b by the image shown in a, using masking as described in the text.

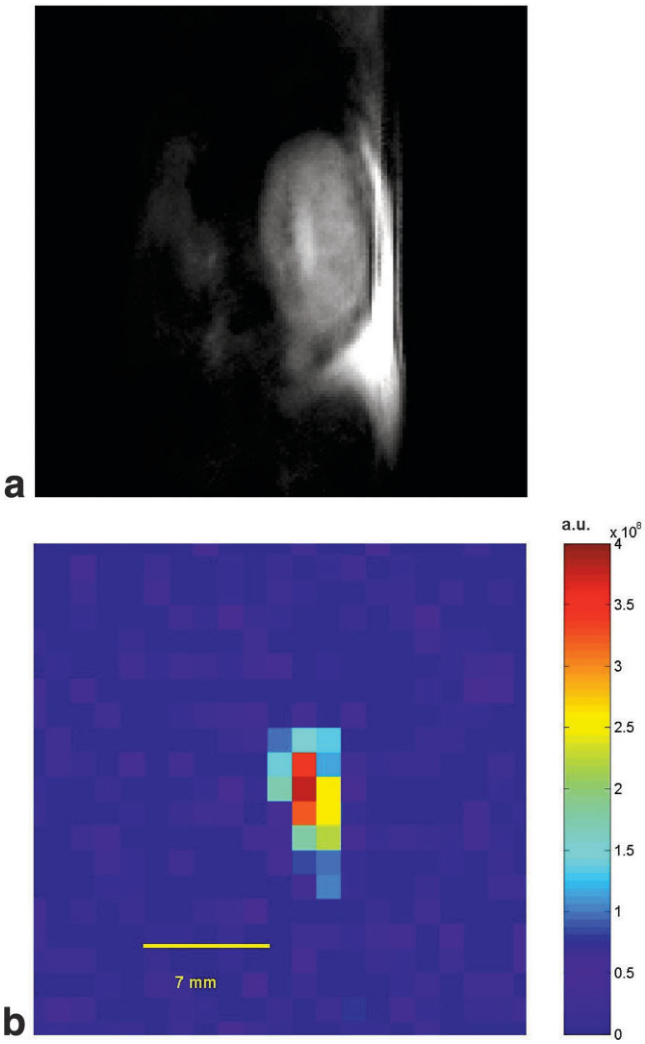

FIG. 3. (**a**). Image of the mouse kidney, at the location used for the MRS and MRSI experiments. FSE with eight encoded echoes per excitation, slice thickness = 2 mm, 256 × 256 matrix, TR = 2.2 s, effective TE = 70 ms, with NEX = 3 applied in an outer loop for reduction of motion artifacts. (**b**) BPA intensity map derived from the SI imaging experiment, by integrating over the aromatic BPA peak areas in the individual, phase-corrected and B_0-aligned spectra.

images in Fig. 2a and b to disappear in an image that represents the ratio between the BPA and water images. Such an image is seen in Fig. 2d, superimposed on the conventional MRI of the selected slice, shown in Fig. 2c. The ratio was calculated only in voxels in which the water intensity exceeded 15% of its maximum and assigned to zero elsewhere. Apparently, the distribution of the ratio values is not entirely homogeneous, and there is a trend for higher values close to the surface coil, suggesting that the integral of the BPA signal may be underestimated as the S/N ratio becomes worse. The BPA/water ratio expected for this experiment is given by

$$\frac{S_{\mathrm{BPA}}}{S_{\mathrm{H_2O}}} = \frac{C_{\mathrm{BPA}}}{C_{\mathrm{H_2O}}} \frac{2(1 - \exp(-\mathrm{TR}/T_1(\mathrm{BPA}))}{(1 - \exp(-\mathrm{TR}/T_1(\mathrm{H_2O}))}. \quad [2]$$

Assuming C_{BPA} = 65 mM, C_{H2O} = 55 M, T_1(BPA) = 1.0 s, and $T_1(H_2O)$ = 3.2 s, then for TR = 1.07 s (used in this experiment), one expects a signal ratio of 5.5×10^{-3}. The possible influence of different T_2 decay for the water and BPA signals was again neglected, its effect expected to be smaller than for the LASER experiment, due to the shorter TE. The *J*-coupling modulation for a second echo at TE = 12 ms should be negligible. In view of the fact that the high values in the distribution in Fig. 2d approach the expected value of 5.5×10^{-3}, and the tendency for the lower values at larger distances from the surface coil, it is likely that the integration of the BPA resonances underestimates their true area for lower S/N ratios.

BPA Detection in a Mouse Kidney

Figure 3a shows a T_2-weighted image of one of the mouse kidneys, and Fig. 3b shows the spectroscopic BPA image at the same location. The SI acquisition was started 73 min after starting the i.v. infusion of the BPA–F solution (and 18 min after the termination of this infusion). The ratio between this image and the corresponding water image was used to calculate a concentration map for BPA. The calculation was based on the empiric average ratio obtained for the 65 mM phantom solution (see above), assuming that the T_1 for BPA was the same as in the phantom, while the T_1 for water was 1.83 s, as measured in situ, and the values therefore represent a molar concentration in the liquid volume fraction of the tissue. The essential part of this BPA concentration map is shown in Fig. 4, superimposed on the anatomic image.

The spectrum of a single central voxel (volume = 9 μL) from this SI data is shown in Fig. 5a. It appears, from the chemical shift of the two prominent peaks, and from the separation between them, that most of the in vivo BPA is in the free form, as opposed to the BPA–F complex in the injected solution. The spectrum shown in Fig. 5b is the

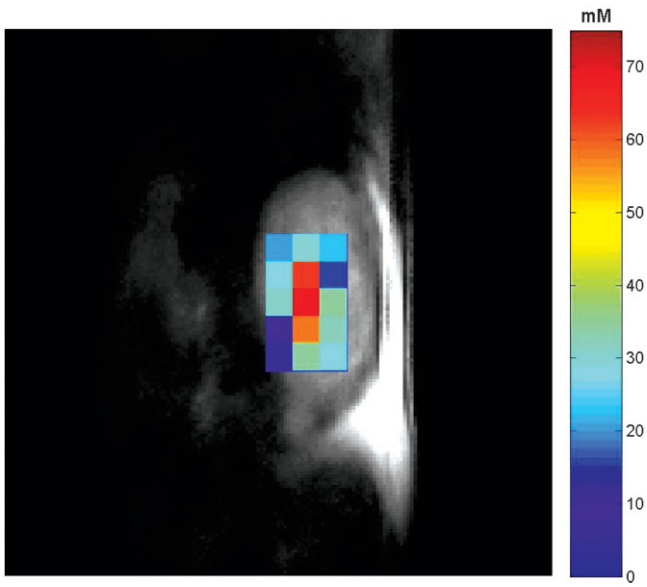

FIG. 4. BPA concentration map (in millimoles per liter liquid, as indicated with the color bar), derived from dividing the BPA by the water intensity map, superimposed on the FSE kidney image.

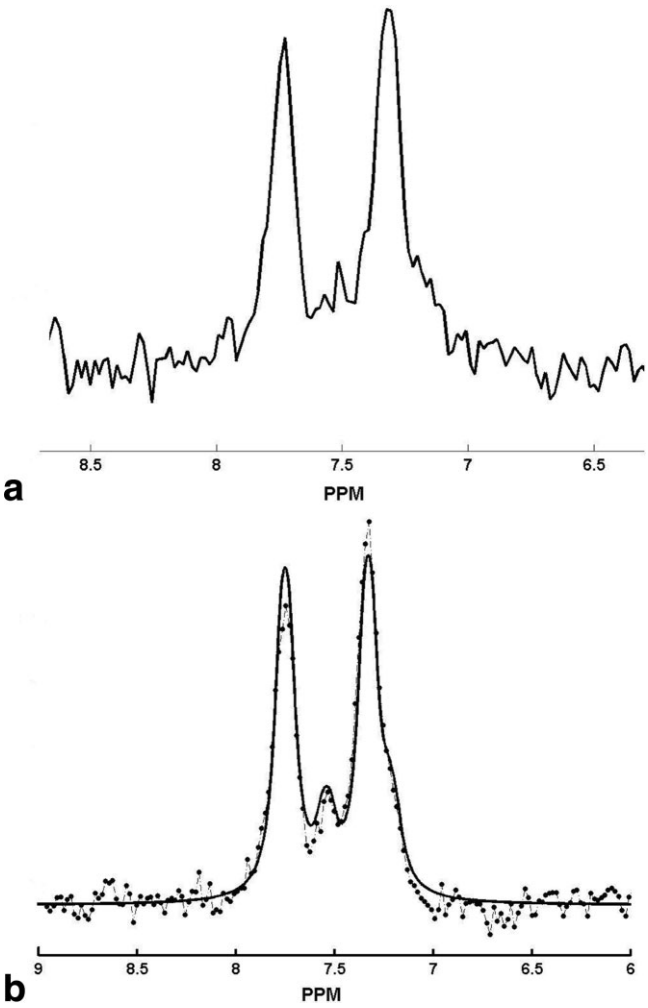

FIG. 5. (**a**). Spectrum of one of the voxels in the kidney, from the SI experiment for BPA. The chemical shift scale was calibrated by setting the water peak to 4.70 ppm. (**b**) Dots (connected by the dot–dash line) indicate the experimental spectrum obtained by summing over 12 voxels covering the kidney from the BPA SI experiment. Solid line: the simulated spectrum, using simulation parameters as indicated in the text.

sum of 12 single-voxel spectra covering most of the kidney in the selected slice, after correcting the frequency scale for each spectrum according to the B_0 in each voxel derived from the water SI map. The spectral resolution for this 108-μL volume is comparable to the single-voxel resolution (Fig. 5a). Superimposed on the experimental spectrum is a simulation, conducted with the following parameters: 80% free BPA with two doublets at chemical shifts 7.33 ppm, 7.75 ppm, *J*-coupling = 7.8 Hz + 20% BPA–F complex with two doublets at chemical shifts 7.21 ppm, 7.54 ppm, and the same *J*-coupling. The simulated peaks were convoluted with a Lorentzian broadening of $\Delta\nu_{1/2}$ = 18 Hz.

LASER spectra, using the acquisition parameters described under Methods, were acquired before, during, and following termination of the BPA infusion. Three such spectra are shown in Fig. 6, at the time points indicated. The voxel size was 146 μL, covering most of the kidney, with dimensions of 5.2 × 7 mm in the plane used for the SI experiments and 4 mm perpendicular to this plane (corresponding approximately to the 4.55-mm slice thickness used for the SI data). The spectrum acquired at 65 min preceded the acquisition of two consecutive SI experiments (for BPA and water), while the spectrum at 105 min was acquired just after these experiments. Apparent average BPA concentrations for the detected voxel were derived, as described under Methods, and corresponded to 67 mM for the top spectrum and 22 mM for the bottom spectrum. The significant decrease of the BPA signal intensity in the kidney was probably due to clearance of the material to the bladder.

DISCUSSION

The ability for quantitative, noninvasive mapping of BPA (or other boronated agents) is important for the successful clinical application of BNCT. First, it is crucial to apply the neutron irradiation at a point in time at which the BPA concentration in the tumor is high enough for best therapeutic results, but at the same time the concentration in blood and surrounding tissue should be low enough to prevent substantial radiation damage to these regions. Second, it is important to know the absolute boron concentrations at the time of irradiation, since these are needed to calculate the radiation dose absorbed by the patient. So far, on-line, real-time measurements of BPA tissue distribution were not applied in clinical treatment protocols. The closest approach to this goal was the use of PET for the detection of ^{18}F-labeled BPA, during "rehearsal" pretreatment uptake and washout experiments (12,13), based on the assumption that the uptake pattern will be quantitatively reproducible (in space and time) during the "real " treatment session. While it is relatively straightforward to test for the boron levels in blood, using various spectroscopic methods, only NMR appears to be capable of performing

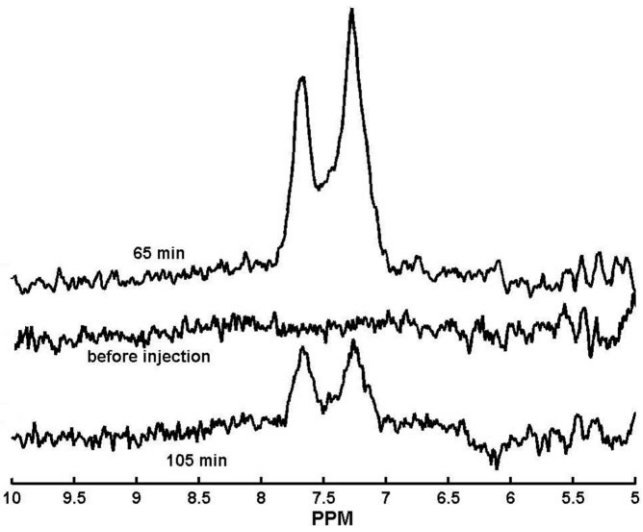

FIG. 6. Three LASER spectra of a 146-μL voxel within the kidney, obtained at different times before and after the beginning of BPA administration, as indicated. The spectra were processed with exponential sensitivity enhancement (LB = 2 Hz).

the relevant in situ measurements during the time between the start of the infusion of the BPA agent and the start of the neutron irradiation, with the intention of increasing treatment efficiency and safety.

Averaged BPA concentration in brain tumors during treatment could reach values of up to ~ 4 mM (14), and should therefore be amenable to clinical ^{1}H MRS detection. Post- minus preinfusion difference spectra can suppress endogenous signals in the same spectral region. Although standard MRS techniques, such as PRESS or STEAM, are capable of detecting BPA, this work demonstrated modified methods that could maximize the efficiency for such detection. Since the signals of the aromatic protons of BPA are split by scalar coupling, our strategy was to reduce the effective TE (or τ_{CP}) as much as possible, using full spin echoes, while maintaining a high degree of robustness and artifact reduction that are usually achieved by the use of longer echo times or stimulated echoes. This was achieved by incorporating, along with the spatially selective pulses, a chemical-shift-selective pulse, focused on the spectral region of the aromatic BPA protons. These principles were implemented in two experiment types with clinical relevance for BPA detection: a single-voxel sequence, for relatively rapid localized spectroscopy of a larger volume, and a 2D, slice-selective, spectroscopic imaging sequence with longer performance time, but capable of providing the spatial distribution of the metabolite over many voxels. The MRSI experiment has the additional advantage of providing the possibility for retrospective trade-off between sensitivity and spatial resolution: as was demonstrated here, the spectra of individual voxels can be averaged over space, providing higher S/N ratio (at the expense of reduced spatial resolution), while maintaining almost the same spectral resolution as in the single voxels, due to the B_0 corrections applied in each of the voxels separately. Although such spatial averaging over N voxels is $(N)^{1/2}$ times less sensitive than single-voxel acquisition over the same volume, part of this loss could be offset by the increased sharpness of the peaks. Finally, while all these procedures were aimed at the in vivo detection of BPA, they are obviously applicable to all cases were J-coupled signals are detected and coverage of a narrow chemical shift range is sufficient.

As opposed to direct ^{10}B detection (2), or ^{10}B-^{1}H double resonance methods (15), which need additional nonstandard hardware, ^{1}H MRS is available on the majority of high-field clinical MRI scanners. Although the BPA concentrations and signal levels, expected in tumor or brain tissue of patients undergoing BNCT, are much lower than in the in vivo example shown here, they are still comparable to the concentrations of other endogenous metabolites detected by ^{1}H MRS. It is therefore hoped that ^{1}H MRS methods such as those demonstrated here could have an impact in the clinical application of BNCT.

ACKNOWLEDGMENTS

Y.S. is the incumbent of the Tillie and Charles Lubin Professorial Chair in Biochemical Endocrinology.

REFERENCES

1. Barth RF. A critical assessment of boron neutron capture therapy: an overview. J Neurooncol 2003;62:1–5.
2. Bendel P, Koudinova N, Salomon Y. In vivo imaging of the neutron capture therapy agent BSH in mice using ^{10}B MRI. Magn Reson Med 2001;46:13–17.
3. Zuo CS, Prasad PV, Busse P, Tang L, Zamenhof RG. Proton nuclear magnetic resonance measurement of *p*-boronophenylalanine (BPA): a therapeutic agent for boron neutron capture therapy. Med Phys 1999; 26:1230–1236.
4. Heikkinen S, Kangasmäki A, Timonen M, Kankaanranta L, Häkkinen A-M, Lundbom N, Vähätalo J, Savolainen S. ^{1}H MRS of a boron neutron capture therapy ^{10}B-carrier, L-*p*-boronophenylalanine-fructose complex, BPA-F: phantom studies at 1.5 and 3.0T. Phys Med Biol 2003;48: 1027–1039.
5. Timonen M, Kangasmäki A, Savolainen S, Heikkinen S. ^{1}H MRS phantom studies of BNCT ^{10}B-carrier, BPA-F using STEAM and PRESS MRS sequences: detection limit and quantification. Spectroscopy 2004;18: 133–142.
6. Tká[caron]c I, Star[caron]cuk Z, Choi I-Y, Gruetter R. In vivo ^{1}H NMR spectroscopy of rat brain at 1 ms echo time. Magn Reson Med 1999;41: 649–656.
7. Geppert C, Dreher W, Leibfritz D. PRESS-based proton single-voxel spectroscopy and spectroscopic imaging with very short echo times using asymmetric RF pulses. MAGMA 2003;16:144–148.
8. Silver MS, Joseph RI, Hoult DI. Highly selective $\pi/2$ and π pulse generation. J Magn Reson 1984;59:347–351.
9. Garwood M, DelaBarre L. The return of the frequency sweep: designing adiabatic pulses for contemporary NMR. J Magn Reson 2001;153:155–177.
10. Geen H, Freeman R. Band-selective radiofrequency pulses. J Magn Reson 1991;93:93–141.
11. Allerhand A. Analysis of Carr-Purcell spin-echo NMR experiments on multiple-spin systems. I. The effect of homonuclear coupling. J Chem Phys 1966;44:1–9.
12. Kabalka GW, Smith GT, Dyke JP, Reid WS, Longford CPD, Roberts TG, Reddy NK, Buonocore E, Hubner KF. Evaluation of fluorine-18-BPA-fructose for boron neutron capture therapy treatment planning. J Nucl Med 1997;38:1762–1767.
13. Imahori Y, Ueda S, Ohmori Y, Kusuki T, Ono K, Fujii R, Ido T. Fluorine-18-labelled fluoroboronophenylalanine PET in patients with glioma. J Nucl Med 1998;39:325–333.
14. Coderre JA, Chanana AD, Joel DD, Elowitz EH, Micca PL, Nawrocky MM, Chadha M, Gebbers JO, Shady M, Peress NS, Slatkin DN. Biodistribution of boronophenylalanine in patients with glioblastoma multiforme: Boron concentration correlates with tumor cellularity. Radiat Res 1998;149:163–170.
15. Bendel P, Zilberstein J, Salomon Y. In vivo detection of a boron neutron capture therapy agent in melanoma by proton-observed ^{1}H-^{10}B double resonance. Magn Reson Med 1994;32:170–174.